

APPLICATION OF GRANULATED BLAST FURNACE SLAG TO REDUCE THE SEISMIC EARTH PRESSURE

Hiroshi MATSUDA, Wonjin BAEK, Daisuke HASHIGUCHI

Yamaguchi University

Haruhiko SHINOZAKI

Nippon Slag Association

ABSTRACT: Granulated Blast Furnace Slag (GBFS) is produced in the manufacture process of pig-iron and shows a similar particle formation as a natural sand. GBFS also shows light weight, high shear strength, well permeability and especially a latent hydraulic property by which GBFS hardens like a rock.

When GBFS is used as a backfill material placed behind such as quay wall, the increase of shear strength induced by the hardening is presumed to reduce the earth pressure and consequently the construction cost of such as harbor structures decreases.

In this study, the model wall tests were carried out on GBFS, in which the resultant earth pressure, a wall friction and the earth pressure distribution at the wall surface were measured, and the test results were compared with those of Toyoura standard sand. In the tests, the relative density was set as $D_r=25, 55$ and 70% and the wall was tilted from vertical to the active earth pressure side and followed by the passive side. The maximum horizontal displacement at the top of the wall was set as $\pm 2\text{mm}$.

By these model tests, it is clarified that the resultant earth pressure obtained by using GBFS is smaller than Toyoura sand, especially in the active-earth pressure side.

KEYWORDS: granulated blast furnace slag, latent hydraulic property, earth pressure

1. INTRODUCTION

Granulated Blast Furnace Slag (GBFS) shows a similar particle formation as natural sand and also shows light weight, high shear strength, well permeability and a latent hydraulic property by which GBFS is solidified (Matsuda et al., 2004). When GBFS is used as a backfill material placed behind such as quay wall and retaining wall, the increase of shear strength induced by the latent hydraulic property is presumed to reduce the earth pressure and the construction cost of the harbor structures decreases.

In this study, by using the sand box (50cm×50cm×100cm) the model wall tests were

carried out on GBFS, in which the resultant earth pressure, wall friction and the earth pressure distribution at the wall surface were measured, and the test results were compared with those of Toyoura standard sand.

In a series of tests, GBFS was uniformly pored into the sand box with a relative density $D_r=25, 55$ and 70% , and then the wall was tilted cyclically for four cycles to the active-side and the passive-side until the wall top displacement reached $\pm 2\text{mm}$ (the positive sign indicates the movement to the passive earth pressure direction and the negative sign indicates to the active earth pressure direction) with the rate of 0.01mm/s . Furthermore, the model tests were also carried out under the earthquake condition

with the horizontal seismic intensity $k_h=0.05, 0.1, 0.15, 0.2$ and 0.3 .

2. SAMPLES AND TEST PROCEDURE

As a sample, GBFS (which is passed through 2mm sieve) and Toyoura sand (Japanese standard sand) were used. Table 1 and Fig.1 show the physical properties, the internal friction angle and the grain size distribution curves. As shown in Table 1, although the specific gravity of GBFS and Toyoura sand are almost the same, the maximum and the minimum void ratio of GBFS is larger than those of Toyoura sand, and the internal friction angle for GBFS with the same relative density $Dr=50\%$ is larger than that of Toyoura sand. This reason is considered that GBFS has a lot of air bubbles in a particle and also the particle shape is squarish.

Figs.2(a), (b) show the tri-axial test results for GBFS with $Dr=25\%$ and 50% . In the tri-axial test,

Table 1 Physical properties and the internal friction angle of samples.

	ρ_s (g/cm^3)	e_{max}	e_{min}	ϕ ($^\circ$)
Toyouira Sand	2.640	0.991	0.630	37.4($Dr=50\%$)
GBFS	2.643	1.51	1.033	37.0($Dr=25\%$) 39.5($Dr=50\%$)

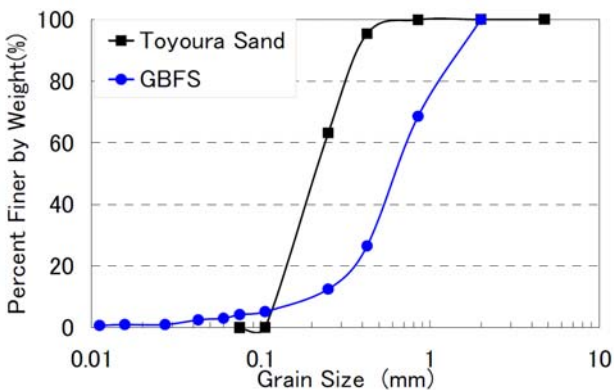


Figure 1 Grain size distribution curve.

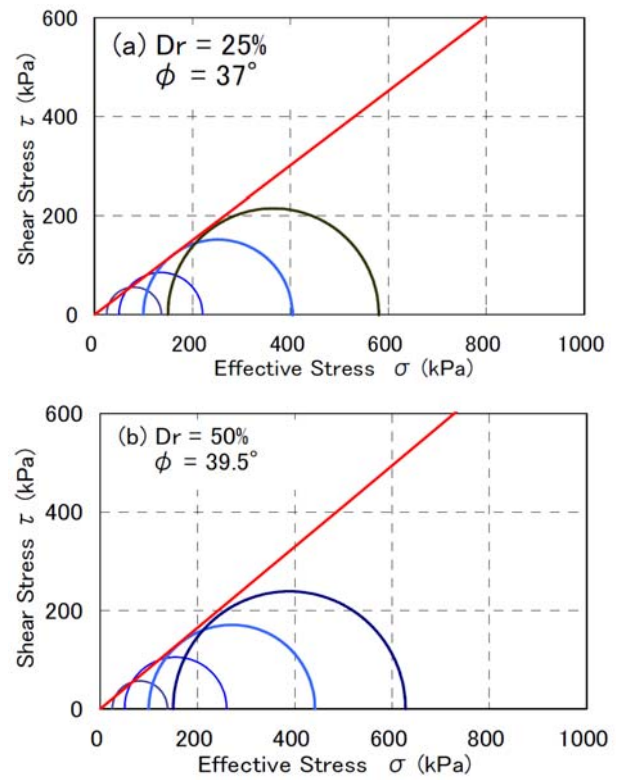


Figure 2 Tri-axial test results on GBFS.

the confining pressure was set as 25, 50, 100 and 150kPa. The sand box is 100cm in length, 50cm in width and 50cm in depth. Fig.3 shows the schematic diagram of sand box (Ohara and Matsuda, 1985). As shown in Fig.3, the wall was supported by the five load transducers which were placed at the bottom end of the wall and also at the top center of the wall, by which the horizontal and the wall friction were measured. Furthermore, three earth pressure transducers were set on the wall surface at

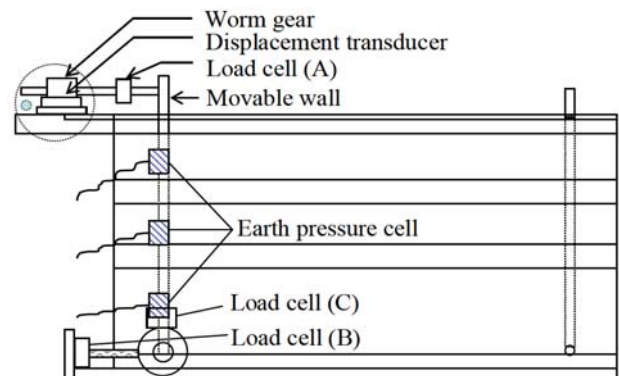


Figure 3 Schematic diagram of sand box. (Ohara and Matsuda, 1985)

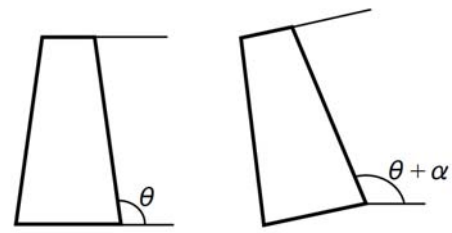
10cm, 25cm and 40cm from the wall top, respectively. The wall was rotated at the predetermined rate around the bottom end of the wall.

3. TEST METHOD

Table 2 shows the test conditions applied in this study. The sample was pored into the sand box and to satisfy the predetermined relative density the volume of the sample was confirmed every 5cm/layer. The average dry unit weight of Toyoura sand was $\gamma=13.78, 14.51\text{kN/m}^3$, for $D_r=25$ and 55% respectively. For GBFS, the average dry unit weight was $\gamma=10.82, 11.48, 11.96\text{kN/m}^3$ for $D_r=25\%$, 55% and 70%.

Fig.4 shows the conceptual diagram to measure the static and the seismic earth pressure, in which the seismic earth pressure is assumed to act on the wall by tilting the sand box to the inclination angle α . Then the seismic intensity k_h is obtained as $k_h = \tan^{-1} \alpha$. In this study, the seismic intensity k_h was changed as 0.05, 0.1, 0.15, 0.2 and 0.3.

For the static condition, after filling the sample in the sand box, the wall was tilted with the rate of



(a) Static condition (b) Earthquake condition

Figure 4 Conceptual diagram to measure the static and the seismic earth pressure.

0.01mm/s until the displacement of the wall top reached -2.0mm. Continuously, the wall was tilted with same rate in the opposite direction until the displacement reached +2.0mm, and then the wall top was moved to the starting position. These operations were repeated for 4 cycles.

For the measurement of seismic earth pressure, after filling GBFS in the sand box, one end of the sand box base was lifted to satisfy the predetermined seismic intensity. Then the wall was tilted as same as the static earth pressure measurement.

4. RESULTANT EARTH PRESSURE AND WALL FRICTION

Figs.5(a), (b) show the relationships between the resultant earth pressure and the displacement of the wall top for Toyoura sand with $D_r=25(\pm 3), 55(\pm 1)\%$.

From these figures, it is seen that the resultant earth pressure for both the active and the passive earth pressure increases with the number of displacement cycles. This reason is considered that the unit weight increases due to the compaction of the particle near the wall. In addition, it is also seen that the static earth pressure reaches the active state when the displacement of the wall top decreased to -0.8mm. In this study, the value of the active earth pressure was defined at the wall top displacement with -2.0mm.

Table 2 Test conditions

GBFS						
Relative Density (%)	Seismic intensity k_h					
	0	0.05	0.1	0.15	0.2	0.3
25	●	●	●	●	-	-
55	●	●	●	●	●	●
75	●	-	-	-	-	-
Toyoura sand						
Relative Density (%)	Seismic intensity k_h					
	0	0.05	0.1	0.15	0.2	0.3
25	●	●	●	●	-	-
55	●	●	●	●	●	●

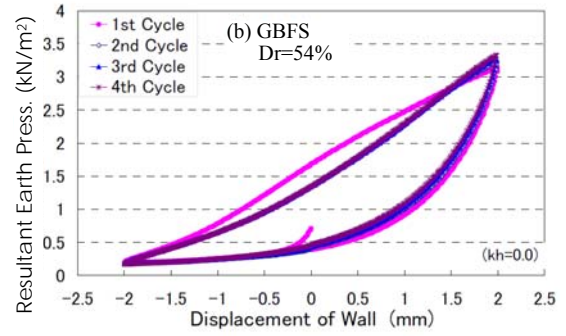
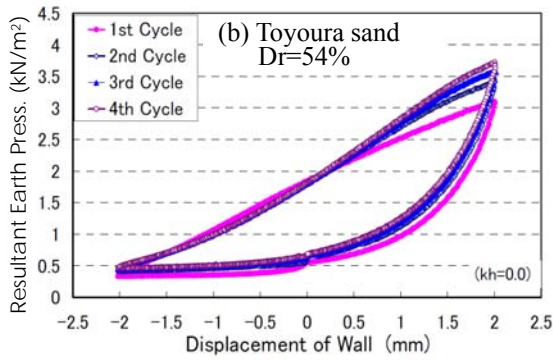
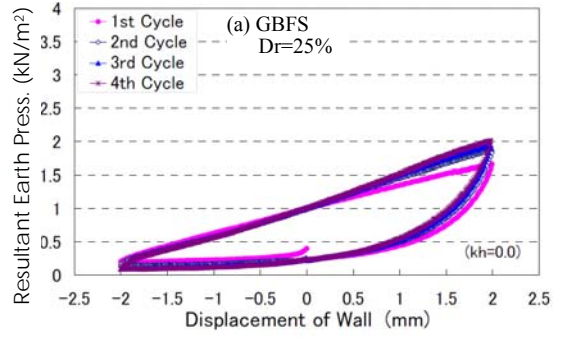
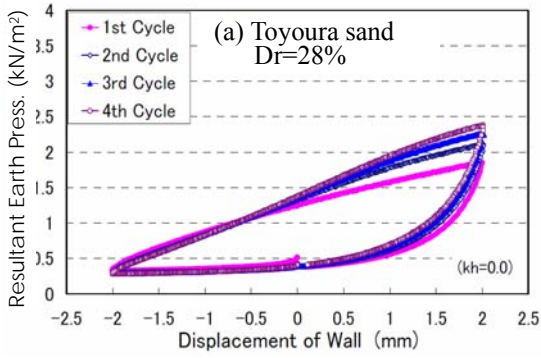


Figure 5 Relations between the resultant earth pressure and the displacement of wall on Toyoura sand.

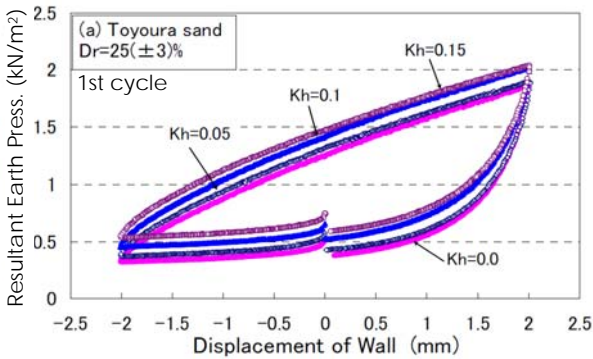
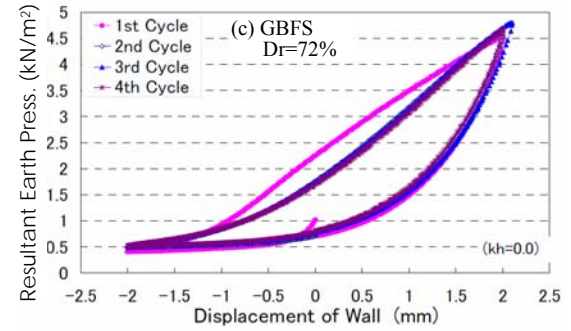
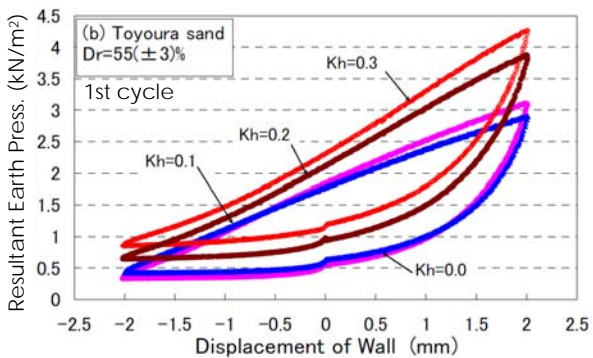


Figure 7 Relations between the resultant earth pressure and the displacement of wall on GBFS.



From these figures, the resultant seismic earth pressure for both the active-side and the passive-side is larger than that of the static earth pressure.

Figure 6 Seismic earth pressure on Toyoura sand.

Figs.6(a), (b) show the relationships between the resultant seismic earth pressure and the seismic intensity k_h for Toyoura sand with $Dr=25, 55\%$.

Figs.7(a), (b), (c) show the change in the resultant earth pressure on GBFS with $Dr=25, 55$ and 70% . From these figures, the resultant static earth pressure increases with the relative density. This is due to the interlocking effect by the angular shape of GBFS and the increase of the unit weight. In addition, the earth pressure becomes smaller in the active-side with the increase of displacement cycles and it becomes larger in the passive-side.

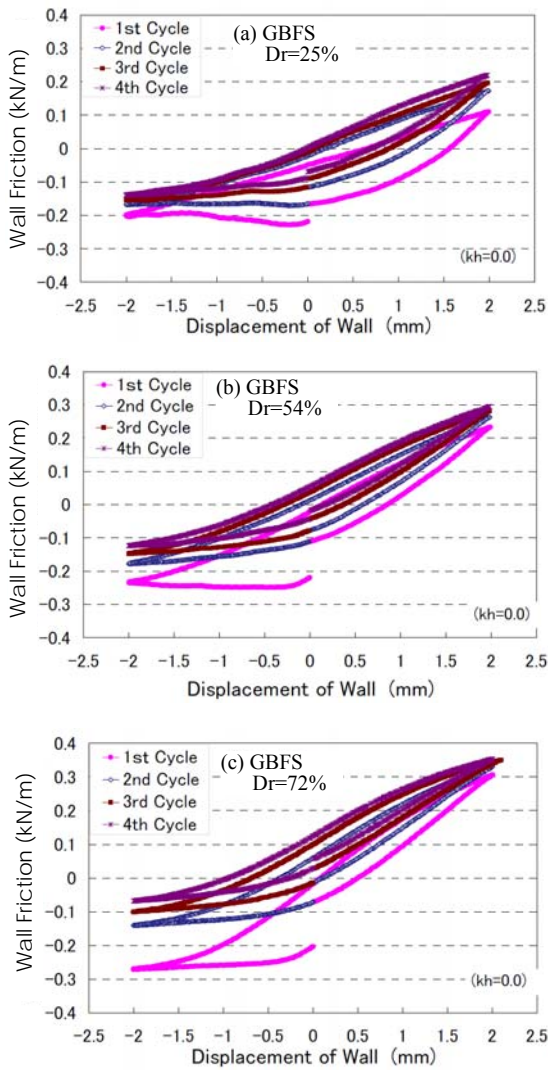


Figure 8 Relationships between the wall friction and the wall displacement on GBFS.

Figs.8(a), (b), (c) show the relationships between the wall friction and the displacement of the wall top for GBFS with $Dr=25$, 55 and 70% . The tendency of the wall friction in the active-side is almost the same for $Dr=25$ and 55% . In the passive-side, however, it increases with the increase of relative density.

Figs.9(a), (b) show the relationships between the resultant earth pressure and the displacement of wall top at the first cycle. As shown in these figures, since GBFS has a lot of air bubbles in a particle and lightweight, and also has a high internal friction angle due to the angular particle shape, the resultant earth pressure of GBFS for both the active-side and the passive-side is smaller than that of Toyoura sand.

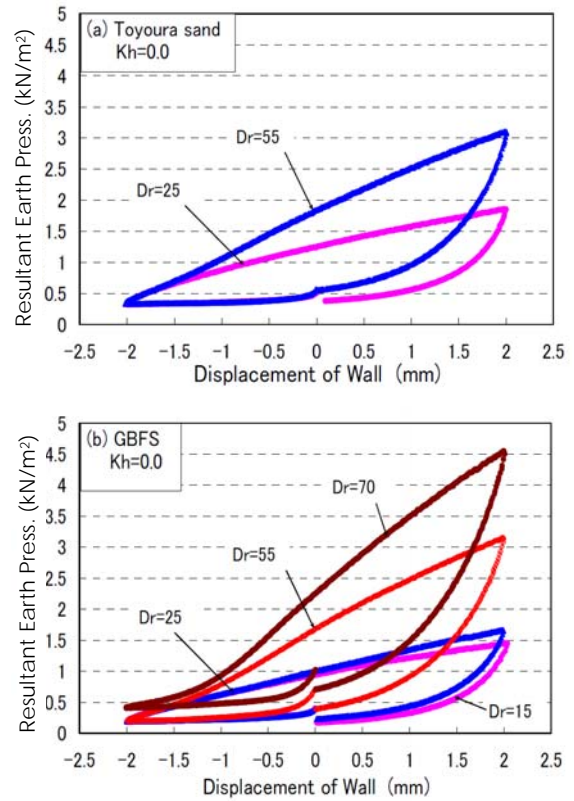


Figure 9 Resultant earth pressure on Toyoura sand and GBFS in static condition.

This means GBFS is applicable as a back-fill material such as quay wall and retaining wall.

Figs.10(a), (b), (c) show the relations between the resultant seismic earth pressure and the wall displacement for GBFS with $Dr=55\%$. The resultant earth pressure for each seismic intensity is larger than the static condition and with increase in the seismic intensity, the resultant earth pressure increases in the active and passive sides.

Figs.11(a), (b) show the relationships between the resultant seismic earth pressure and the seismic intensity k_h for GBFS with $Dr=25$ and 55% . The seismic earth pressure for the active-side and the passive-side increases with the seismic intensity for both relative densities.

Fig.12 shows the relationships between the resultant active earth pressure and the seismic

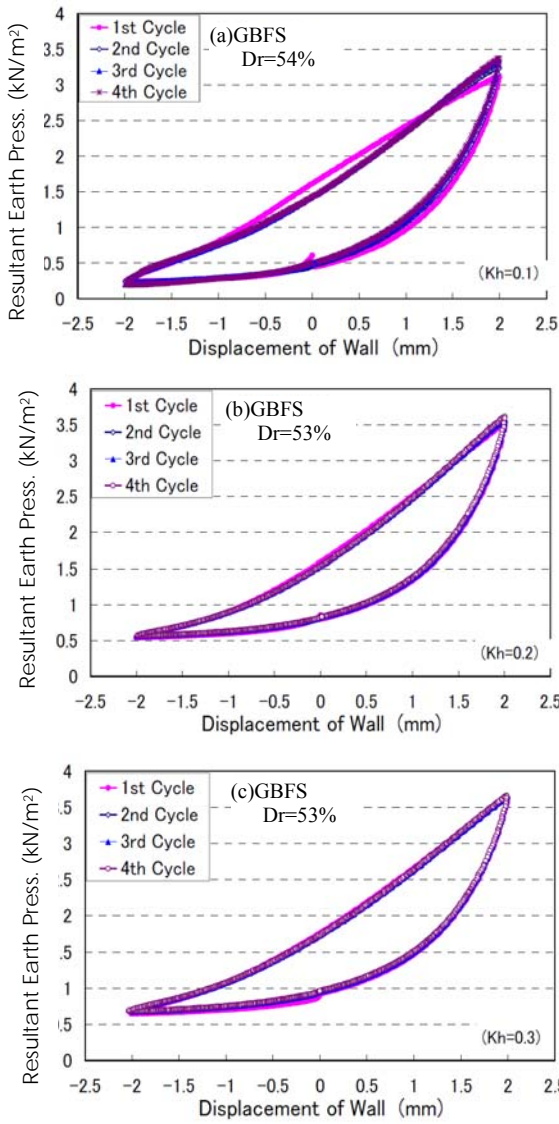


Figure 10 Seismic earth pressure on GBFS (Dr=55%).

intensity. For Toyoura sand and GBFS, the resultant earth pressure increases with the seismic intensity and the resultant earth pressure of GBFS is smaller than that of Toyoura sand.

5. CONCLUSIONS

In this study, by using the sand box, a series of the model wall tests for the static and the seismic conditions were carried out on the Granulated Blast Furnace Slag (GBFS), in which the resultant earth pressure, the wall friction and the earth pressure distribution at the wall surface were measured, and the test results were compared with those of Toyoura

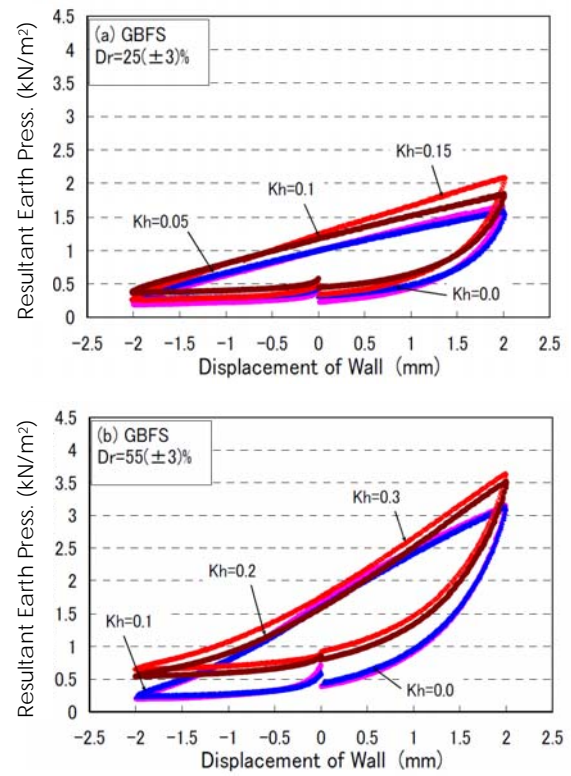


Figure 11 Seismic earth pressure on GBFS.

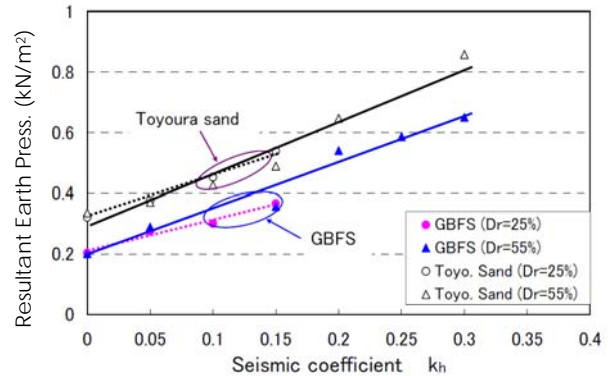


Figure 12 Relationships between total horizontal earth pressure and seismic coefficient.

sand. The main conclusions are summarized as follows.

- (1) A smaller resultant earth pressure was obtained for GBFS compared with the Toyoura sand for the relative density in the range from 25 – 55%.
- (2) The resultant earth pressure in the active side decreases with the number of displacement cycles for both GBFS and Toyoura sand. In the

passive side, the resultant earth pressure increases with the displacement cycles.

- (3) For GBFS and Toyoura sand, the resultant earth pressure and the wall friction in the static and seismic condition increase with the relative density.

REFERENCES

Matsuda H., N. Kitayama, K. Takamiya, T. Murakami and Y. Nakano : Study on granulated blast furnace slag applying to the ground improvement, *Journal of the Japan Society of Civil Engineers*, Vol.764, III-67, pp.85-99, 2004.

Ohara, S. and H. Matsuda : Calculation of seismic earth pressure acting on quay wall, *Journal of the Japan Society of Civil Engineers*, Vol.358, III-3, pp.103-111, 1985.